Korean J. Chem. Eng., 33(4), 1159-1169 (2016)
DOI: 10.1007/s11814-015-0256-y

pISSN: 0256-1115
eISSN: 1975-7220

Heat transfer of bio-oil in a direct contact heat exchanger during condensation

Hoon Chae Park, Hang Seok Choi†, and Ji Eun Lee

Department of Environmental Engineering, Yonsei University, Wonju 26493, Korea
(*Received 7 May 2015 • accepted 26 November 2015*)

Abstract−Rapid quenching of volatiles in fast pyrolysis is important for achieving high yield and quality of the bio-oil product, but few studies have examined the condensation of volatiles and their related heat exchangers. Accordingly, we have studied the condensation characteristics of volatiles by varying heat transfer conditions in a direct contact heat exchanger. As the mass flow rate ratio of quenching oil to pyrolysis gas increased, the heat transfer rate and yield of bio-oil increased. The heat transfer rate and yield of bio-oil reached a maximum value at an intermediate air-to-quenching oil mass flow rate ratio. Additionally, the heat transfer rate and yield of bio-oil decreased as the temperature of the quenching oil increased. Experiments were also conducted to derive an empirical relationship for the volumetric heat transfer coefficient for direct contact heat exchangers.

Keywords: Bio-oil, Direct Contact Heat Exchanger, Fast Pyrolysis, Heat Transfer

INTRODUCTION

The current reliance on fossil fuels contributes to environmental problems, such as climate change, air pollution, and resource depletion. Hence, as an alternative energy source, bio-energy has gained much attention. Some thermochemical conversion methods have been developed to convert biomass into energy, such as direct combustion, gasification, and pyrolysis. Many studies have focused on the fast pyrolysis of biomass, through which biomass is decomposed into useful compounds in the liquid, solid, and gas states by using a combination of heat and O_2-free conditions [1]. This fast pyrolysis process produces bio-oil, which can be directly used for generating heat and power [2]. However, this process has many specific requirements, including appropriate pyrolysis temperature, rapid heating rate, short residence time of volatiles, and rapid condensation of volatiles [3]. Although the most appropriate fast pyrolysis temperature varies according to the type of biomass, temperatures in the range of 400 to 500 °C are generally applied [4]. Fast pyrolysis also requires a rapid heating rate that is more than 1,000 °C/s [5]. To minimize the cracking of volatiles into non-condensable gas or char via secondary reactions, the reactors must limit the residence time of volatiles to less than 2 s [6]. Additionally, volatiles should be rapidly condensed to maintain the bio-oil yield [7]. In bio-oil production, the rapid condensation of volatiles is one of the most important requirements. Both the time that volatiles reside in the reactor and the temperature at which the volatiles condense influence the composition and quality of the bio-oil products.

Direct and indirect contact heat exchangers are widely used for various commercial purposes. During the fast pyrolysis process, volatiles can be quenched by a direct or indirect contact heat exchanger. Direct contact heat exchangers have a number of advantages over the indirect, including simpler design, lower capital and maintenance costs, higher specific heat transfer areas, and higher heat transfer rates [8]. In the fast pyrolysis process, serious plugging problems can occur when certain indirect contact heat exchangers, such as the shell and tube heat exchanger, are used. These plugging problems can hinder steady and continuous operation. Hence, several types of direct contact heat exchangers are used in the fast pyrolysis process. Few studies, however, have investigated the condensation characteristics of different direct contact heat exchangers for the quenching of fast pyrolysis volatiles. Understanding the condensation heat transfer and the consequent performance of heat exchangers is important for designing a highly efficient heat exchanger and predicting its performance. However, the complex physical phenomena that accompany gas-solid multiphase flows have hindered studies on the condensation of volatiles in the fast pyrolysis process. Most studies have focused on the effects of condensation temperature on the yield and physicochemical characteristics of bio-oil. For instance, Zhang et al. [9] and Asadullah et al. [10] connected heat exchangers in series to collect volatiles and study the yield and physicochemical characteristics of bio-oil, whereas Salehi et al. [11] and Boateng et al. [12] examined the yield and moisture content of bio-oil according to condensation temperature. Westerhof et al. [13] used a direct contact heat exchanger to study the moisture content of bio-oil after varying the condensation temperature, the volume of volatiles, and the moisture content of the samples. Lu et al. [14] and Zheng et al. [15] used hybrid heat exchangers that combined direct contact heat exchangers with a shell and tube heat exchanger to examine changes in kinematic viscosity according to the temperature of the condensed bio-oil, in addition to variations of kinematic viscosity and moisture content over storage time. Direct contact heat exchangers include single and fractional (i.e., multi-step) heat exchangers. Fractional heat exchangers result in two streams with well-defined boiling point distributions. For example, the first step heat exchanger oper-

†To whom correspondence should be addressed.
E-mail: hs.choi@yonsei.ac.kr

ates between 40 and 90 °C, and the second step heat exchanger operates between 20 and 30 °C [16]. Fractional heat exchangers have been used in the initial separation step in fast pyrolysis processes for upgrading bio-oil into fuels and chemicals [17]. Recently, Karlsson and Nilsson [18] and Gustavsson and Nilsson [19] studied the co-production of bio-oil in district heating plants using fractional heat exchangers. Karlsson and Nilsson [18] investigated the potential of utilizing waste heat from bio-oil heat exchangers for district cooling. Gustavsson and Nilsson [19] evaluated the impact of pyrolysis integration into plants in terms of pyrolysis oil production, power generation, biomass consumption, and overall energy efficiency.

The majority of studies on fast pyrolysis have focused on optimizing the characteristics of fast pyrolyzers to increase the yield and quality of bio-oil [20,21]. However, the condensation process itself is also an extremely important aspect to consider when designing a fast pyrolysis plant. To minimize secondary reactions and maximize oil yields, volatiles must be quenched very rapidly. However, our knowledge regarding volatile condensation after fast pyrolysis is incomplete owing to the complicated physical phenomena involved in this process. In this study, we examined the condensation heat transfer characteristics of volatiles while using a direct contact heat exchanger. In particular, we aim to derive the volumetric heat transfer coefficient of a direct contact heat exchanger, which will be required for the optimal design of direct contact heat exchangers in a full-scale plant.

MATERIALS AND METHODS

1. Materials

In this study, fast pyrolysis of larch sawdust was performed. A standard sieve (ASTM E-11-61) was used to separate larch particles according to size; particles of 1-2 mm size were used. To remove the initial moisture, the raw material was dried in an oven at 105± 5 °C for 24 h. The physical and chemical properties of the raw material are given in Table 1; the physicochemical characteristics of bio-oil, which were collected after the fast pyrolysis of larch sawdust, are given in Table 2. Table 2 shows the characteristics of bio-oil condensed under the following conditions: $\dot{m}_{air}/\dot{m}_{qo}$=0.2, $\dot{m}_{qo}/\dot{m}_{g}$=4, and a quenching oil temperature of 45 °C. The characteristics of bio-oil change according to the operating conditions of the direct contact heat exchanger. Sufficient bio-oil was not available for us to use in the direct contact exchanger during the initial stage of operation. Therefore, process oil that can be used instead of the bio-oil was required. For the direct contact heat exchanger, paraffin process oil, which does not dissolve in bio-oil, was selected as the quenching oil. The characteristics of paraffin process oil are shown in Table 3.

Table 1. Characteristics of the raw material (larch particles)

Particle size (mm)	1-2
Bulk density (kg/m^3)	314
High heating value, HHV (MJ/kg)	16.52
Proximate analysis (wt%)	
Water	3.19
Volatile	78.58
Fixed carbon	17.09
Ash	1.15
Ultimate analysis (dry basis wt%)	
C	47.12
H	6.00
O	46.77
N	0.11
S	-

Table 2. Characteristics of the bio-oil

Moisture content (wt%)		5.96
Density (kg/m^3)		1260
Elemental composition (wt%)	C	56.25
	H	10.18
	N	-
	O	33.5
LHV (MJ/kg)		21.61
Viscosity (mPa·s, at 50 °C)		115.9
pH		2.7
Solids (wt%)		0.03
Ash content (wt%)		0.002

* Condensation conditions: $\dot{m}_{air}/\dot{m}_{qo}$=0.2, $\dot{m}_{qo}/\dot{m}_{g}$=4, Quenching oil temperature=45 °C

Table 3. Quenching oil characteristics

Product type		Hydrocarbon mixture (Mineral oil)
Hydrocarbon element	Paraffin, %	65
	Naphthene, %	34
	Aromatic, %	1
Solubility in water		Negligible
Pour point (°C)		210
Density (kg/m^3)		862
Specific heat (kJ/kg-K)		1.884
Kinematic viscosity (mm^2/s, at 20 °C)		30.2
Lower heating value, LHV (MJ/kg)		47.31

2. Experimental Method

The experimental apparatus for the fast pyrolysis system, which used a bubbling fluidized bed reactor, is shown in Fig. 1. In this apparatus, a silo containing larch particles, and two screw feeders of identical size and configuration supplied larch particles into the bubbling fluidized bed reactor. The upper feeder controlled the feed rate of larch particles, and the lower one transported them into the fluidized bed reactor. The reactor was constructed of stainless steel (SUS-304) and its diameter and height were 70 mm and 210 mm, respectively. The reactor was filled with 320 g of silica sand and heated with an electric heater to maintain the reaction temperature at 500 °C for fast pyrolysis. The residence time of the gas stream, including permanent gases and volatiles, was less than

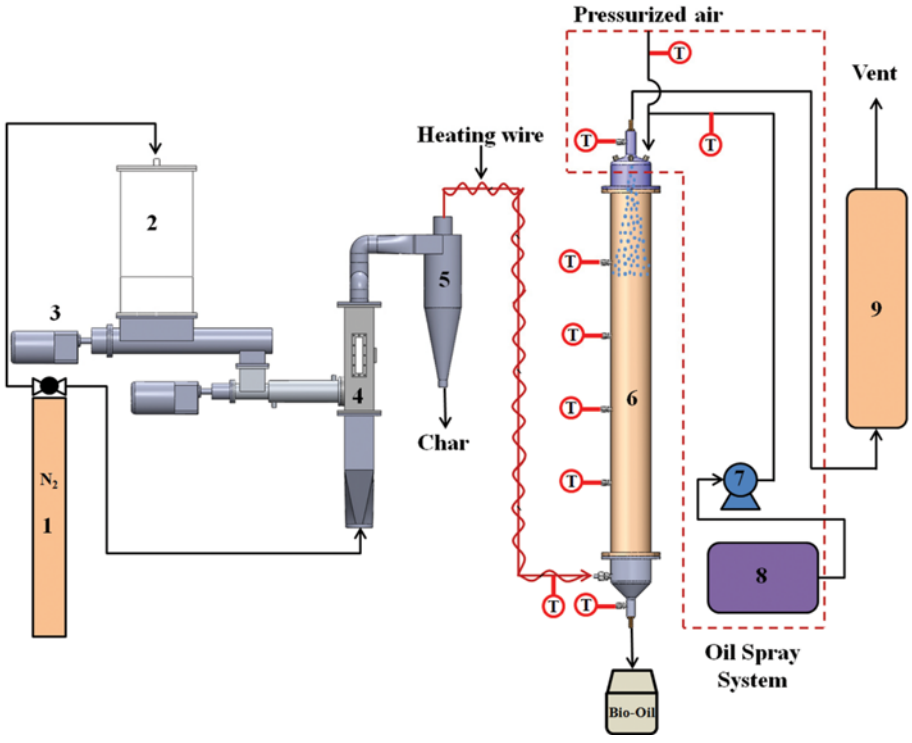

Fig. 1. Schematic diagram of the experimental apparatus.

1. N_2 gas vessel
2. Silo
3. Screw feeder
4. Bubbling fluidized bed reactor
5. Cyclone
6. Direct contact heat exchanger
7. Oil pump
8. Chiller
9. Electrostatic precipitator

2 s. A cyclone separated and collected the char particles that were dispersed in the gas stream. The volatiles were condensed by cold paraffin oil droplets in a direct contact heat exchanger before collection of the condensed bio-oil. An electrostatic precipitator was used to trap the fine oil mist before it reached the vent.

To enable the observation of condensation phenomena, the direct contact heat exchanger was made of transparent acryl. Its diameter was 150 mm, and the height was 1,000 mm. Two air atomizer nozzles were placed on the head of the heat exchanger for atomizing and spraying paraffin oil over the incoming gas stream. The oil spray system consisted of a chiller, an oil pump, and spraying nozzles. The temperature of the quenching oil was controlled by the temperature controller of the chiller. The atomizer nozzle generated fine oil droplets to increase their contact surface. The specifications of the nozzle are given in Table 4. To measure the temperatures of the gas stream and quenching oil, K-type thermocouples were placed at the inlet and outlet of the heat exchanger. Four additional thermocouples were also installed at regular intervals inside the heat exchanger. To prevent the condensation of volatiles before reaching the heat exchanger [22], pipe lines between the reactor and the heat exchanger were heated to above 240 °C.

Table 4. Specifications of the atomizer nozzle

Spray type	Full cone
Spray angle	20°
Material	Stainless steel
Manufacturer	Hanmi Nozzle, Korea

The experimental conditions for the fast pyrolysis of larch particles and direct contact condensation are listed in Table 5. The fast pyrolysis parameters were chosen to maximize the yield of bio-oil and were obtained from previous experiments [23,24]. A single fraction of bio-oil contains water from the process as well as all of the chemical compounds that are found in fast pyrolysis bio-oil. The goal of fractionating bio-oil is to separate the bio-oil into distinct fractions that contain different families of chemical compounds. A single or fractional heat exchanger can be used, depending on the final purpose of the bio-oil. A fractional heat exchanger can be used for upgraded bio-oil or in connection with district heating [25]. However, a single heat exchanger can be used for co-combusting the bio-oil in a boiler in an economical way [25]. The purpose of this study was to produce bio-oil at a low price without additional equipment because it focuses on producing bio-oil for

Table 5. Experimental conditions for the fast pyrolysis of larch particles and direct contact condensation

Fast pyrolysis	Pyrolysis temperature (°C)	500
	Particle size (mm)	1-2
	N_2 flow rate (L/min)	20
	Larch particle feeding rate (g/min)	3.3
Direct contact condensation	$\dot{m}_{qo}/\dot{m}_g$	1, 2, 3, 4
	$\dot{m}_{air}/\dot{m}_{qo}$	0.1, 0.2, 0.3, 0.4
	Quenching oil temperature (°C)	15, 25, 35, 45

co-combustion in a boiler. To achieve this goal, operating the heat exchanger at the ambient temperature can be economical. Therefore, the condensation temperature was selected as 15-45 °C. The mass flow rate ratios of the quenching oil to the pyrolysis gas ($\dot{m}_{qo}/\dot{m}_g$) are given in Table 5. In these ratios, the mass flow rate of the quenching oil was varied, while that of the pyrolysis gas was maintained at a constant value. The mass flow rate of the pyrolysis gas ($\dot{m}_g$) was calculated from the bio-oil mass ($m_{bio\text{-}oil}$), char mass (m_{char}), feeding time (t_{feed}), and raw material mass (m_{feed}) as

$$\dot{m}_g = \frac{m_g}{t_{feed}}, \quad m_g = m_{feed} - (m_{bio\text{-}oil} + m_{char}). \tag{1}$$

To determine the influence of the ratio $\dot{m}_{qo}/\dot{m}_g$ and quenching oil temperature, the ratio $\dot{m}_{qo}/\dot{m}_g$ and quenching oil temperature were varied during the experiments, while the ratio $\dot{m}_{air}/\dot{m}_{qo}$ was fixed at 0.2. Hence, the atomizing performance and droplet size of the nozzle were almost the same in all cases. In the ratio $\dot{m}_{air}/\dot{m}_{qo}$, the air mass flow rate was varied, while that of the quenching oil was fixed.

Direct contact condensation is initiated when the temperatures of the reactor and quenching oil are stably maintained. Bio-oil, which is condensed in the direct contact heat exchanger, is collected as a mixture of bio-oil and quenching oil in a conical flask at the bottom of the heat exchanger. A mixture of bio-oil (ρ=1,260 kg/m^3) and quenching oil (ρ=860 kg/m^3) is shown in Fig. 2(a). After a certain period of time, the mixture separates into two layers according to density, as shown in Fig. 2(b).

3. Calculation of the Heat Transfer Coefficient

The volumetric heat transfer coefficient (U_V) of a direct contact heat exchanger is defined as [26]

$$U_V = \frac{Q}{V\Delta T_{lm}}, \tag{2}$$

where Q is the heat transfer rate, V is the volume of the direct contact heat exchanger, and ΔT_{lm} is the log mean temperature difference. The heat transfer rate (Q) is the summation of all latent heat (released or absorbed during the phase change of the volatiles) and sensible heat (transferred by the temperature differences). Heat loss from the heat exchanger to the outside was assumed to be negligible; additionally, heat transfer was assumed to occur only among the pyrolyzed gas stream, air, and quenching oil. The rate of heat loss from the pyrolysis gas was equal to the rate of heat gain by the quenching oil and the air that was injected through the spray nozzle. Under these assumptions, based on the first law of thermodynamics [26], the heat released from the pyrolyzed gas stream can be expressed as

$$\begin{aligned} Q &= \underbrace{Q_{g,\,latent} + Q_{g,\,sensible}} = \dot{m}_g h_{fg} + \dot{m}_g C_{p,\,g}(T_{g,\,in} - T_{g,\,out}) \\ &= \sum_{i=1}^{n} \dot{m}_{vi} h_{fgi} + (\dot{m}_g - \dot{m}_v) Y_j \sum_{j=1}^{m} C_{p,\,ncgj}(T_{ncgj,\,in} - T_{ncgj,\,out}) \end{aligned} \tag{3a}$$

where subscript v indicates volatile gas, ncg indicates non-condensable gas, i represents the species of the volatile gas, and j represents the species of the non-condensable gas. Additionally, the heat absorbed by the quenching oil and air can be expressed as

$$\begin{aligned} Q &= \underbrace{Q_{qo} + Q_{air}} \\ &= \dot{m}_{qo} C_{p,\,qo}(T_{qo,\,out} - T_{qo,\,in}) + \dot{m}_{air} C_{p,\,air}(T_{qo,\,out} - T_{qo,\,in}) \end{aligned} \tag{3b}$$

The volumetric heat transfer coefficient was calculated by measuring the heat transfer rates and the log mean temperature differences:

$$\Delta T_{lm} = \frac{\Delta T_1 - \Delta T_2}{\ln(\Delta T_1/\Delta T_2)}, \quad \Delta T_1 = T_{g,\,in} - T_{qo,\,out}, \quad \Delta T_2 = T_{g,\,out} - T_{qo,\,in}. \tag{4}$$

The heat transfer rates of the quenching oil and the air were calculated by measuring the mass flow rates of the quenching oil and the air injected from the nozzle as well as the inlet and outlet temperatures of the quenching oil and air. These parameters were measured at the top and bottom of the direct contact heat exchanger. The quenching oil and the condensed bio-oil were mixed and then drained into the bottom of the direct contact heat exchanger. The air and non-condensed gases were also mixed and released from the top of the direct contact heat exchanger. Measuring the individual temperatures of fluids in a mixed state is technically challenging. Therefore, the mixed fluids were assumed to be in thermal equilibrium at the inlet and outlet. The air and quenching oil released from the nozzle were also assumed to have the same temperature.

The latent heat and specific heat capacity are essential parameters in the design of heat exchangers. Only limited reports are available on the specific heat capacity. According to Lu et al. [27], the specific heat capacity of bio-oil may be 2.5-3.5 kJ/kg-K in the temperature range of 20-60 °C. The latent heat of bio-oil, calculated with the heat capacity and Eq. (3a), is 840 kJ/kg. For reference, Zhang [28] studied the latent heat of chemical components of bio-oil. According to Zhang's results, the latent heat ranges from 481 to 1,159 kJ/kg. Hence, the calculated value of the latent heat can be considered reasonable.

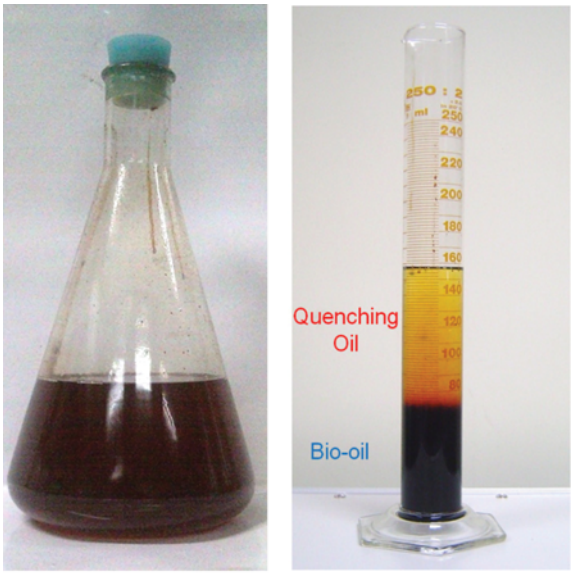

Fig. 2. Collected oil mixture.
(a) Oil mixture (b) Separated oils

4. Measurement of Quenching Oil Droplet Diameter

A droplet size analyzer (Malvern Spraytec) was used to measure the diameters of the quenching oil droplets released from the atomizer nozzles. The analyzer (see Fig. 3) consisted of a He-Ne

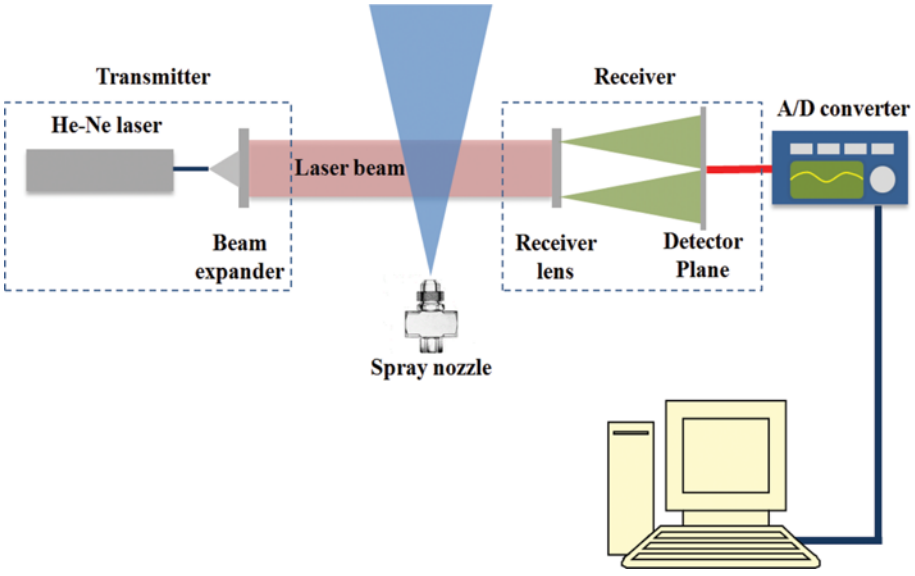

Fig. 3. Schematic diagram of the Malvern droplet size analyzer.

laser, transmitter, and receiver module. The laser beam passed through the spray at an axial distance of 100 mm from the nozzle tip. The laser beam was expanded to 10 mm in diameter by the transmitter and diffracted when it passed through the spray. A receiver lens with a focal length of 750 mm was used, thereby allowing the measurement of droplets of size ranging from 2.0 μm to 1.5 mm. The diffracted light was received by the detector plane through a Fourier lens and transferred to a digital signal by an analog-to-digital (A/D) converter. Finally, a computer calculated the droplet size distribution.

5. Bio-oil Analysis

The water content of the bio-oil was analyzed by Karl Fischer titration, as outlined in ASTM E 203. A Karl Fischer titrator (KF 787 Titrino, Metrohm) was used. The heating value was measured with a calorimetric value (higher heating value, HHV) according to the DIN 51900 Standard. The calorimetric value was determined using a LECO AC 300 calorimeter. Bio-oil viscosity was measured as dynamic viscosity according to ASTM D 4878. The dynamic viscosity was determined at 40 °C with a Brookfield DVII+ Pro Viscometer.

RESULTS AND DISCUSSION

1. Characteristics of Droplet Size Distribution for Quenching Oil

The effects of varying the mass flow rate ratio of air to quenching oil on the droplet size distribution are shown in Fig. 4. The droplet size distributions were measured by maintaining a constant mass flow rate of quenching oil from the nozzle and increasing the mass flow rate of air. As the mass flow rate ratio of air to quenching oil increased, the number of small droplets increased, whereas the number of large droplets decreased. However, this trend was reversed when $\dot{m}_{air}/\dot{m}_{qo}$ was above 0.3. The effects of changing the mass flow rate ratio of air to quenching oil on the Sauter mean diameter (SMD) of the droplets are shown in Fig. 5.

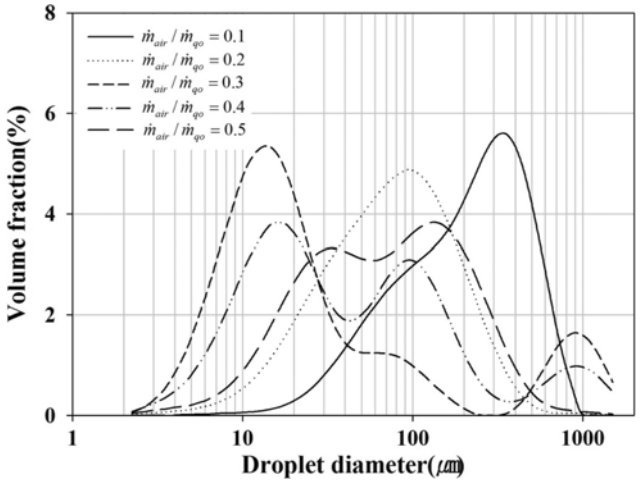

Fig. 4. Distribution of quenching oil droplet diameters for a single nozzle.

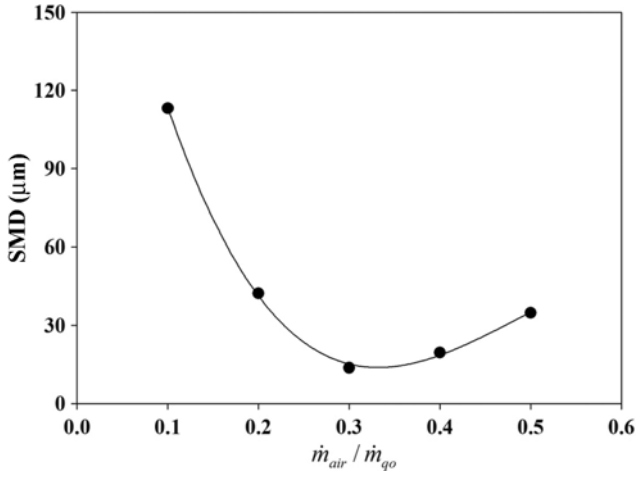

Fig. 5. SMD as a function of $\dot{m}_{air}/\dot{m}_{qo}$.

The minimum droplet SMD (13.6 μm) occurred when the mass flow rate ratio was increased to 0.3. However, the droplet SMD increased when the mass flow rate ratio was above 0.3, presumably because of an increased number of large droplets, as shown in Fig. 4. As the ratio $\dot{m}_{air}/\dot{m}_{qo}$ increased from 0.1 to 0.3, the Weber number increased from 114 to 423 and the SMD decreased from 113.1 μm to 13.6 μm. This can be explained as follows. For Weber numbers less than one, the surface tension dominates the atomization process, but inertial forces dominate for Weber numbers greater than one. Below a Weber number of 10, atomization is dominated by inertial forces and bag breakup occurs. Above a Weber number of 10, shear breakup occurs and results in a very fine spray [29]. However, at Weber numbers above approximately 120, the SMD appears to increase. This suggests that unlike the single-phase spraying nozzle, the two-phase flow atomizer nozzle is affected by the phenomenon whereby the nozzle configuration, such as nozzle tip shape, of the atomizer nozzle influences the spray performance.

2. Effect of Mass Flow Rate Ratio of Quenching Oil to Pyrolysis Gas on Condensation Heat Transfer

The effect of changing the mass flow rate ratio of the quenching oil to pyrolysis gas on the temperature distribution in the direct contact heat exchanger is shown in Fig. 6(a). Hot pyrolysis gas is issued into the direct contact heat exchanger at the bottom inlet of the heat exchanger and flows out through the upper outlet. During the migration of the gas, it exchanges its heat with the quenching oil droplets and air, which are sprayed by the atomizer nozzles located at the top of the heat exchanger. Therefore, the lower part of the direct contact heat exchanger, where the hot gas stream is supplied, has the highest temperature. Furthermore, the upper part of the heat exchanger, where the quenching oil is sprayed, has the lowest temperature. Hence, the temperature decreases from the bottom to the top of the heat exchanger. At all heights in the exchanger, the temperature decreased as the mass flow rate of the quenching oil increased. The heat transfer rates between the gas stream and quenching oil with respect to mass flow rate ratio are shown in Fig. 6(b). The heat transfer rates were calculated with Eq. (3) after the flow rate of the quenching oil, the temperature at the inlet, and the temperature at the outlet were measured. The heat transfer rate increased as the mass flow rate of the sprayed quenching oil increased as shown in Fig. 6(b). This observation is attributable to the increased contact area for heat transfer between the quenching oil and the pyrolysis gas, which is proportional to the mass flow rate of the quenching oil. Thus, the bio-oil yield increases as the mass flow rate of the quenching oil increases as shown in Fig. 7(a). However, as the mass flow rate ratio increased, the heat-

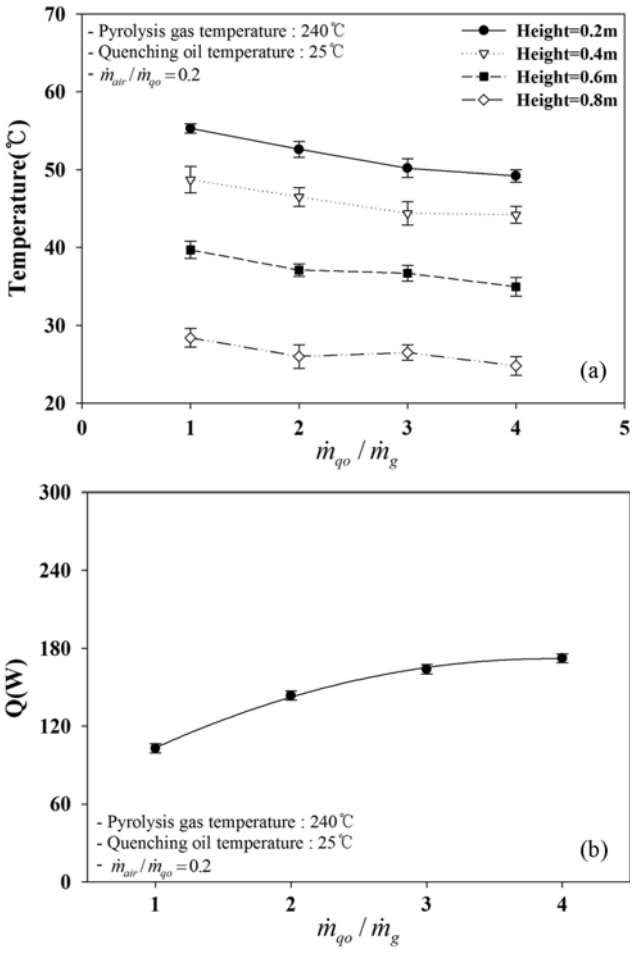

Fig. 6. Heat transfer characteristics of the direct contact heat exchanger as a function of $\dot{m}_{qo}/\dot{m}_g$.
(a) Temperature distributions in the direct contact heat exchanger, (b) Variation of heat transfer rate

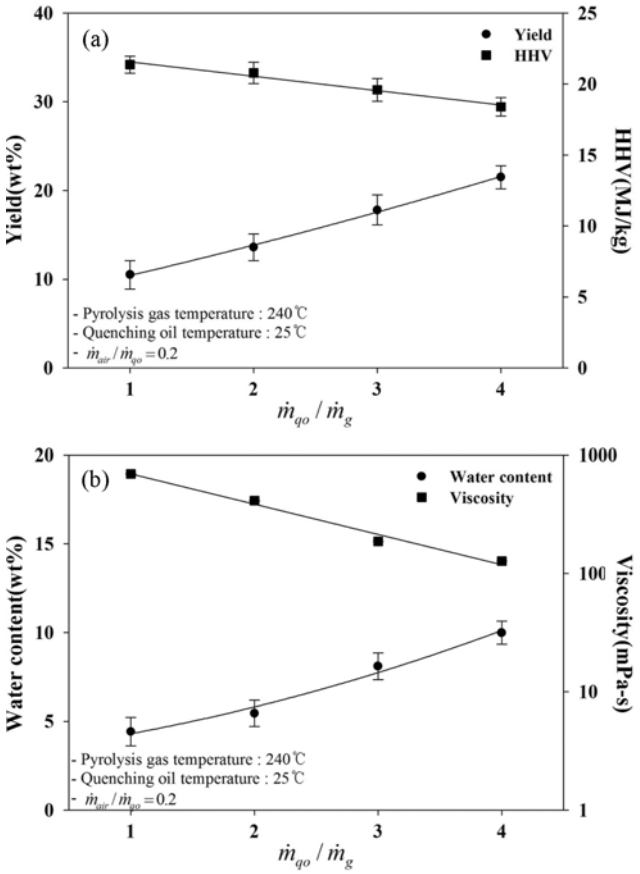

Fig. 7. Effect of $\dot{m}_{qo}/\dot{m}_g$ on the yield and properties of the bio-oil.
(a) Yield and high heating value, (b) Water content and viscosity

Table 6. Product yields of fast pyrolysis in different experimental conditions

	$\dot{m}_{qo}/\dot{m}_g$				$\dot{m}_{air}/\dot{m}_{qo}$				Quenching oil temperature (°C)			
	1	2	3	4	0.1	0.2	0.3	0.4	15	25	35	45
Bio-oil	41.9	52.5	54.3	55.9	48.4	55.9	55.4	50.2	60.5	55.9	47.4	45.9
Non-condensable gas	43.6	34.3	30.6	29.8	37.2	29.8	31.3	34.6	26.1	29.8	37.1	41.4
Char	14.5	13.2	15.1	14.3	14.4	14.3	13.3	15.3	13.4	14.3	15.5	12.7

ing value of the bio-oil decreased from 21.3 MJ/kg to 18.3 MJ/kg. This observation can be explained by Fig. 7(b), which shows the water content and viscosity with respect to $\dot{m}_{qo}/\dot{m}_g$. As the mass flow rate of the quenching oil increased, the water content of the bio-oil increased from 4.4 wt% to 9.9 wt%. This increase resulted in a decreased viscosity and decreased heating value of the bio-oil. Note that this paper presents only the yield of the bio-oil condensed in the direct contact heat exchanger. The total bio-oil, char, and non-condensable gas yields are given in Table 6. In the present experiment, an electrostatic precipitator was installed at the end of the direct contact heat exchanger to collect the oil mist that was not condensed in the direct contact heat exchanger. In the electrostatic precipitator, the bio-oil was collected at 20-30 wt%. For example, at $\dot{m}_{qo}/\dot{m}_g$=4, the bio-oil yield of the direct contact heat exchanger was 21.5 wt%, and that of the electrostatic precipitator was 34.4 wt%. The total yield of 55.9 wt% is close to the previous research result of 57.8 wt% [23]. However, compared with the result of [30], the total bio-oil yield of the present study is lower. This is mainly due to the different fast pyrolysis conditions, especially biomass size, heating rate, residence time, and condensation condition. The yield of char was 14.3 wt%, and the yield of non-condensable gas was 29.8 wt%. These values are comparable to the previous research result of 20.0 wt% char and 23.2 wt% non-condensable gas [23].

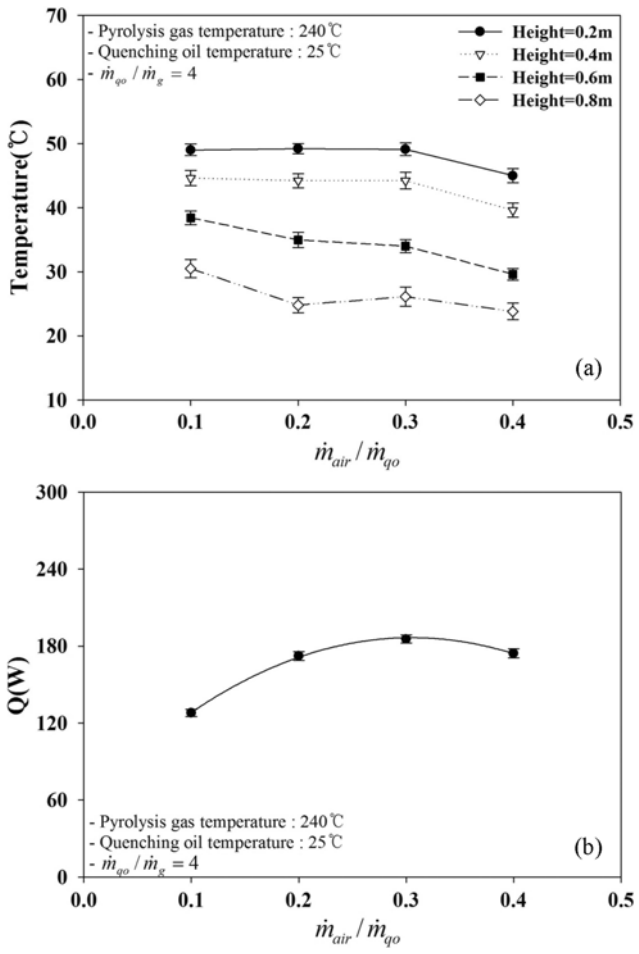

Fig. 8. Heat transfer characteristics of the direct contact heat exchanger as a function of $\dot{m}_{air}/\dot{m}_{qo}$.
(a) Temperature distributions in the direct contact heat exchanger, (b) Variation of heat transfer rate

3. Effect of Air Flow Rate on Condensation Heat Transfer

The temperature distributions inside the direct contact heat exchanger with varying mass flow rate ratio of the quenching oil to air are shown in Fig. 8(a). For mass flow rate ratios ranging from 0.1 to 0.3, the temperatures in the lower part of the exchanger (heights of 0.2 m and 0.4 m) were quite similar. However, as the mass flow rate ratio increased above 0.3, the temperature decreased. In the upper part of the exchanger (heights of 0.6 m and 0.8 m), the temperature gradually decreased as the mass flow rate ratio increased. As the air flow rate increases above a certain limit, heat transfer between the volatiles and the quenching oil has been shown to decrease in direct contact heat exchangers [31]. The heat transfer rate in the direct contact heat exchanger according to the mass flow rate ratio is shown in Fig. 8(b). As the mass flow rate ratio increased, the heat transfer rate also increased because the SMD of the quenching oil decreased. However, when the mass flow rate ratio exceeded 0.3, the heat transfer rate began to decrease. This decrease can be attributed to the decreased contact area for heat transfer between the pyrolysis gas and the quenching oil, as shown in Fig. 4. As the mass flow rate ratio was increased above 0.3, the proportion of large droplets also increased. In addition, since the increased air flow rate boosted the spray velocity of the nozzle, the droplets of the quenching oil rapidly dropped to the lower part of the heat exchanger. This effect may have shortened the residence time of the quenching oil, consequently decreasing the amount of heat transfer between the pyrolysis gas stream and the quenching oil droplets. Finally, changing the amount of heat transfer also affects the condensation of volatiles, resulting in the bio-oil yields shown in Fig. 9(a). The maximum bio-oil yield was obtained at the maximum heat transfer rate. In addition, the maximum HHV was obtained at the maximum bio-oil yield. However, the air flow rate exerted only a small influence on the heating value. The effects of changing the mass flow rates of air and quenching oil on the water content and viscosity of the bio-oil are shown in Fig. 9(b). As $\dot{m}_{air}/\dot{m}_{qo}$ increased, the water content first increased and then decreased. In contrast, the viscosity showed the opposite

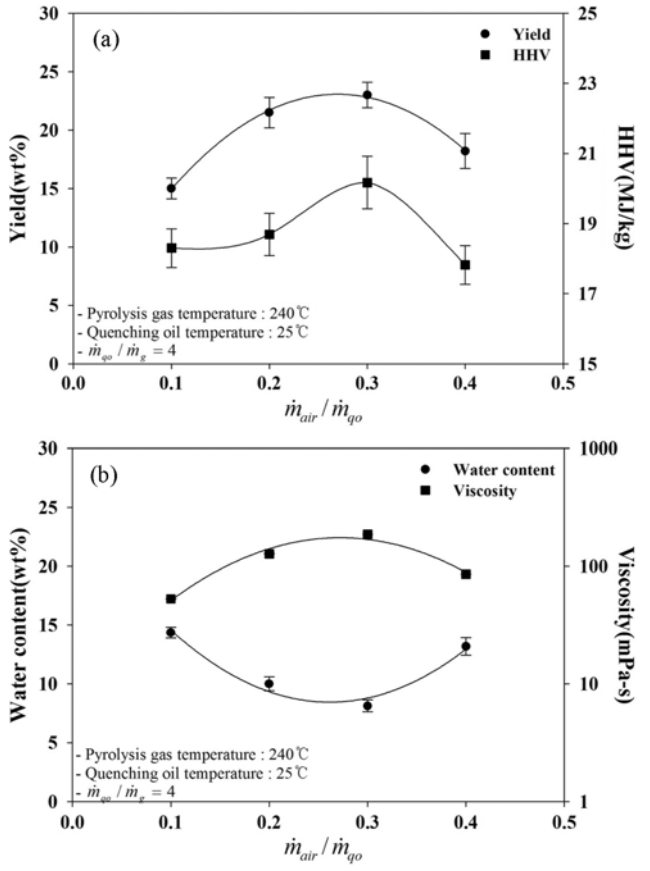

Fig. 9. Effect of $\dot{m}_{air}/\dot{m}_{qo}$ on the yield and properties of the bio-oil.
(a) Yield and heating value, (b) Water content and viscosity

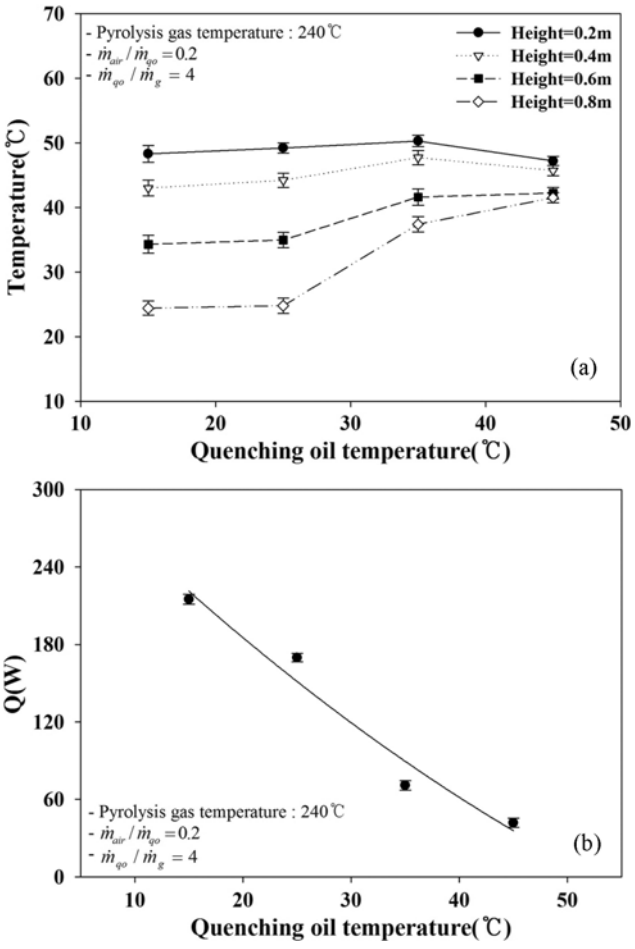

Fig. 10. Heat transfer characteristics of the direct contact heat exchanger as a function of quenching oil temperature.
(a) Temperature distributions in the direct contact heat exchanger, (b) Variation of heat transfer rate

pattern. At $\dot{m}_{air}/\dot{m}_{qo}$=0.3, the water content of the bio-oil was the lowest (8.1 wt%), whereas the viscosity was the highest (186 mPa·s). Interestingly, the water content was inversely proportional to the heat transfer rate as $\dot{m}_{air}/\dot{m}_{qo}$ increased. This finding is quite different from other cases in which $\dot{m}_{qo}/\dot{m}_g$ changes according to the quenching oil temperature. According to reference [32], the water content of bio-oil is directly proportional to the heating value. For example, in the reference, the heating value changes by 43% as the water content changes by 28%. Such a change may affect the condensation of volatiles, but the influence of water content is more significant. However, observing the changes to the ratio $\dot{m}_{air}/\dot{m}_{qo}$ in this study, the heating value increases by 0.5% when the water content decreases by 4.4%, and the changes in the heating value due to changes in water content are less significant than the influence of the condensation temperature, which contrasts the above reference. As shown in Fig. 4, this is attributable to the relationship between the flow characteristics of atomized droplets and condensation. The heating value of bio-oil depends on the water content, oxygen content, and oxygenated compounds. Bio-oil is composed of a complex mixture of oxygenated compounds containing various chemical functional groups, such as carbonyl, carboxyl, and phenolic groups. It consists of the following constituents: 20-25% water, 25-30% water insoluble pyrolytic lignin, 5-12% organic acids, 5-10% non-polar hydrocarbons, 5-10% anhydrosugars, and 10-25% other oxygenated compounds. The presence of oxygenated compounds reduces the heating value of the bio-oil. Because of the complex composition of bio-oil, it is very difficult to analyze the effect of the heavy non-volatile fraction of bio-oil on the heating value. This is worth investigating in the future but is beyond the scope of this study and is therefore excluded.

4. Effect of Quenching Oil Temperature on Condensation Heat Transfer

Fig. 10(a) shows the temperature distribution within the direct contact heat exchanger at various temperatures of the quenching oil supplied to the atomizer nozzle. At each height within the direct contact heat exchanger, the temperature increased as the temperature of the quenching oil increased. However, the temperature slightly decreased in the lower part of the exchanger when the quenching oil temperature was above 40 °C. Moreover, the temperature gradient decreased as the quenching oil temperature increased; this decrease was more significant when the quenching oil temperature exceeded 25 °C. The temperature change was most noticeable in the upper region of the direct contact heat exchanger, where the quenching oil is sprayed. It is noted that for each height, the temperature profile remains almost constant for quenching oil temperatures below 25 °C.

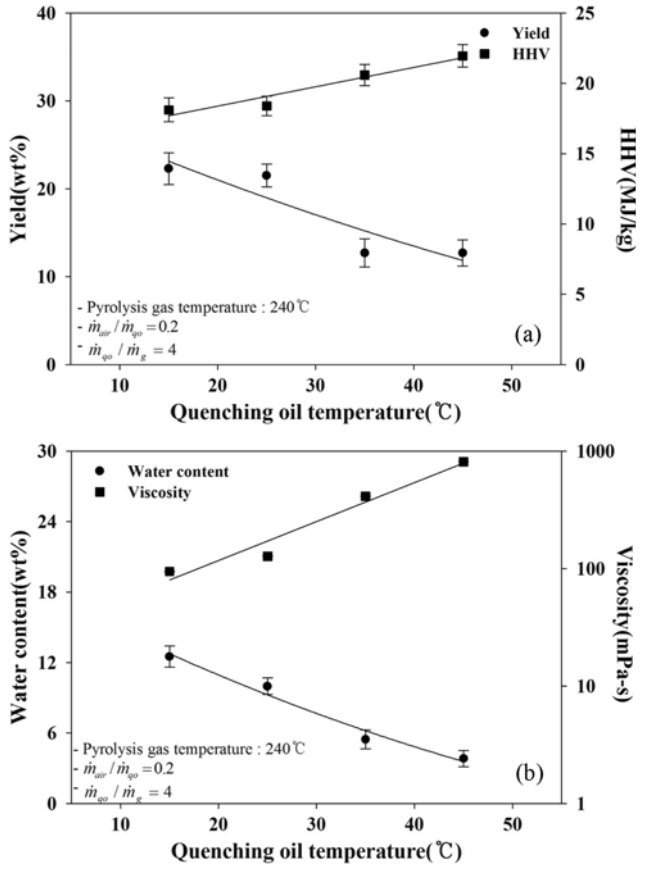

Fig. 11. Effect of quenching oil temperature on the yield and properties of the bio-oil.
(a) Yield and heating value, (b) Water content and viscosity

The heat transfer rate with respect to quenching oil temperature is shown in Fig. 10(b). As the quenching oil temperature increased, the heat transfer rate rapidly decreased. The bio-oil yields and heating values at various quenching oil temperatures are shown in Fig. 11(a). The bio-oil yield was higher at lower quenching oil temperatures. However, as the quenching oil temperature increased, the heating value increased from 18.1 MJ/kg to 21.9 MJ/kg. Fig. 11(a) shows the water content and viscosity with respect to the quenching oil temperature. As the quenching oil temperature increased from 15 °C to 45 °C, the bio-oil water content decreased from 12.5 wt% to 3.8 wt%, respectively, thus increasing the bio-oil viscosity and HHV with increased quenching oil temperatures.

5. Volumetric Heat Transfer Coefficient of the Direct Contact Heat Exchanger

The experimental correlation developed in this study for the volumetric heat transfer coefficient according to superficial liquid mass velocity (L) is shown in Fig. 12. Considering the heat transfer efficacy from Fig. 10(b), the experimental correlation was developed only for the quenching oil temperatures of 15 °C and 25 °C. As shown in Fig. 12, the volumetric heat transfer coefficient of the direct contact heat exchanger increased as the superficial liquid mass velocity increased at the two different quenching oil temperatures. The effect of the quenching oil temperature on the volumetric heat transfer coefficient was relatively small. The experimental

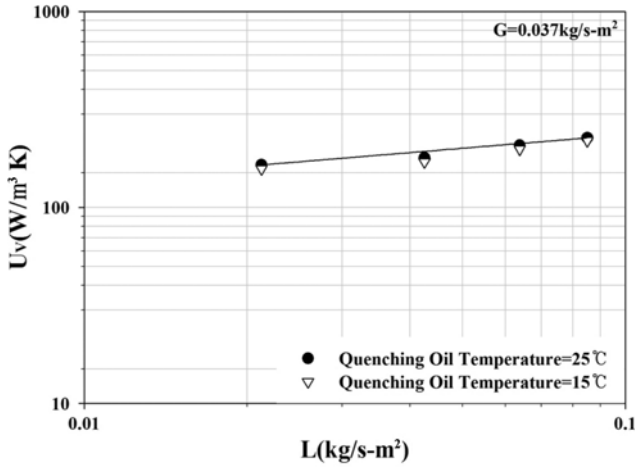

Fig. 12. Empirical correlation formula for the volumetric heat transfer coefficient.

correlation of the volumetric heat transfer coefficient was derived using the least squares method with the mass flow rate ratio as an independent variable. The correlation for the volumetric heat transfer coefficient and its applicable range is

$$U_V=1996G^{0.49}L^{0.23}\begin{cases}0.1\le \dot{m}_{air}/\dot{m}_{qo}\le 0.5\\ 1.0\le \dot{m}_{qo}/\dot{m}_{g}\le 4.0\\ 15\le T_{qo}\le 25\end{cases}. \quad (5)$$

CONCLUSION

We examined the rapid condensation of volatiles in biomass fast pyrolysis by using a direct contact heat exchanger to perform condensation heat transfer experiments. The results from the present study can be summarized as follows.

(1) A particle analyzer was used to measure the quenching oil droplet size. As the air flow rate increased in the atomizer nozzle, the SMD of the sprayed liquid droplets decreased, since the collision velocity of air increased. This increase resulted in a corresponding increase of the contact surface area of the quenching oil. The mean droplet size was approximately 20-90 μm.

(2) The heat transfer rate of the direct contact heat exchanger increased as the mass flow rate of the sprayed quenching oil increased. Increasing the mass flow rate ratio ($\dot{m}_{qo}/\dot{m}_{g}$) from 1 to 4 resulted in an increase in the heat transfer rate from 102 W to 172 W. The increase occurred because the contact area between the volatiles and the quenching oil droplets increased as the mass flow rate of the sprayed quenching oil increased; therefore, both heat and mass transfer were augmented.

(3) As the mass flow rate ratio of air to quenching oil injected through the nozzles increased from 0.1 to 0.3, the heat transfer rate increased because the SMD of the quenching oil decreased. However, when the mass flow rate ratio of air to quenching oil was more than 0.3, the heat transfer rate decreased.

(4) When the temperature of the quenching oil increased, the heat transfer rate from volatiles to the quenching oil decreased because the temperature difference between them decreased. As the

quenching oil temperature increased from 15 °C to 45 °C, the heat transfer rate decreased from 215.1 W to 41.9 W. The quenching oil temperature had little effect on the heat transfer rate at temperatures ranging from 15 °C to 25 °C. However, between 25 °C and 35 °C, the quenching oil temperature significantly affected the heat transfer rate.

(5) An empirical correlation for the volumetric heat transfer coefficient, which is required to design direct contact heat exchangers, was derived and is given in Eq. (6) and Fig. 12.

(6) The yield of condensed bio-oil increased as the heat transfer rate increased. However, the water content showed a different pattern as the mass flow rate ratio of air to quenching oil was varied. The water content of the bio-oil affects both its heating value and viscosity. As the water content increased, the heating value and the viscosity both decreased.

In this study, the heat exchangers were assumed perfectly insulated with no heat loss to the environment, and the effect of the heavy non-volatile fraction of bio-oil on the heating value was not considered. In the future, it would be useful to analyze how the complex composition of bio-oil affects the heating value.

ACKNOWLEDGEMENTS

This work was supported by a National Research Foundation of Korea (NRF) grant funded by the Ministry of Science, ICT, and Future Planning (MSIP) of Korea (No. NRF-2014R1A2A2A03003812).

NOMENCLATURE

C_p : specific heat [J/kg-K]
d : nozzle diameter [m]
G : superficial gas mass velocity [kg/s-m^2]
h_{fg} : condensation latent heat [J/kg]
L : superficial liquid mass velocity [kg/s-m^2]
m : mass [kg]
$\dot{m}$: mass flow rate [kg/s]
Q : heat transfer rate [W]
SMD : Sauter mean diameter
T : temperature [K]
U : overall heat transfer coefficient [W/m^3-K]
u : velocity [m/s]
V : volume [m^3]
We : Weber number
Y : mass fraction

Greek Symbols

ΔT_{lm} : log mean temperature difference
ρ : density [kg/m^3]
σ : surface tension [N/m]

Subscripts

c : condensation
g : pyrolysis gas
in : inlet
out : outlet
qo : quenching oil
t : time
V : volumetric

REFERENCES

1. R. H. Venderbosch and W. Prins, *Biofuels, Bioprod. Biorefin.*, **4**, 178 (2010).
2. S. Czernik and A. V. Bridgwater, *Energy Fuels*, **18**, 590 (2004).
3. A. V. Bridgwater, D. Meier and D. Radlein, *Org. Geochem.*, **30**, 1479 (1999).
4. J. P. Diebold and A. V. Bridgwater, in *Fast Pyrolysis of Biomass: a Handbook*, CPL Press, London (1999).
5. D. Mohan, C. U. Pittman and P. H. Steele, *Energy Fuels*, **20**, 848 (2006).
6. S. H. Jung, B. S. Kang and J. S. Kim, *J. Anal. Appl. Pyrol.*, **82**, 240 (2008).
7. T. Chen, C. Deng and R. Liu, *Energy Fuels*, **24**, 6616 (2010).
8. M. Song, A. Steiff and P. M. Weinspach, *Chem. Eng. Sci.*, **54**, 3861 (1999).
9. H. Zhang, R. Xiao, H. Huang and G. Xiao, *Bioresour. Technol.*, **100**, 1428 (2009).
10. M. Asadullah, M. A. Ali Rahman, M. A. Motin Rahman, M. R. Sultan and M. R. Alam, *Fuel*, **86**, 2514 (2007).
11. E. Salehi, J. Abedi and T. Harding, *Energy Fuels*, **23**, 3767 (2009).
12. A. A. Boateng, D. E. Daugaard, N. M. Goldberg and K. B. Hicks, *Ind. Eng. Chem. Res.*, **46**, 1891 (2007).
13. R. J. M. Westerhof, N. J. M. Kuipers, S. R. A. Kersten and W. P. M. van Swaaij, *Ind. Eng. Chem. Res.*, **46**, 9238 (2009).
14. Q. Lu, X. L. Yang and X. F. Zhu, *J. Anal. Appl. Pyrol.*, **82**, 191 (2008).
15. J. L. Zheng, W. M. Yi and N. N. N. Wang, *Energy Convers. Manage.*, **49**, 1724 (2008).
16. R. J. M. Westerhof, S. R. A. Kersten, M. Garcia-Perez, Z. Wang and W. P. M. Van Swaaij, *Energy Fuels*, **25**, 1817 (2011).
17. L. R. Jarboe, Z. Wen, D. Choi and R. C. Brown, *Appl. Microbiol. Biotechnol.*, **91**, 1519 (2011).
18. V. Karlsson and L. Nilsson, *Appl. Therm. Eng.*, **79**, 9 (2015).
19. C. Gustavsson and L. Nilsson, *Energy Fuels*, **27**, 5313 (2013).
20. H. S. Choi, Y. S. Choi and H. C. Park, *Korean J. Chem. Eng.*, **27**, 1164 (2010).
21. P. Weerachanchai, C. Tangsathitkulchal and M. Tangsathitkulchai, *Korean J. Chem. Eng.*, **28**, 2262 (2011).
22. A. J. S. Pollard, Comparison of Bio-oil Produced in a Fractionated Bio-oil Collection System, Master's Thesis, Iowa State University, Ames, IA (2009).
23. H. S. Choi, Y. S. Choi and H. C. Park, *Renewable Energy*, **42**, 131 (2012).
24. H. C. Park, A Study on Condensation Heat Transfer Characteristics of Bio-crude Oil in Direct Contact Heat Exchanger, Master's Thesis, Chungnam National University, Daejeon, Republic of Korea (2010).
25. M. Garcia-Perez, J. A. Garcia-Nunez, T. Lewis, C. Kruger and S. Kantor, Methods for Producing Biochar and Advanced Bio-fuels in Washington State. Part 3: Literature Review of Technologies for Product Collection and Refining, Third Project Report, Department of Biological Systems Engineering and the Center for Sustaining Agriculture and Natural Resources, Washington State

University, Pullman, WA (2011).
26. A. Bejan and A. D. Kraus, *Heat Transfer Handbook*, Wiley, Hoboken, NJ (2003).
27. Q. Lu, W. Z. Li and X. F. Zhu, *Energy Convers. Manage.*, **50**, 1376 (2009).
28. L. Zhang, *Multicomponent drop vaporization modeling of petroleum and biofuel mixtures*, Doctor's Thesis, Iowa State University, Iowa, USA (2011).
29. J. B. Kennedy, *J. Eng. Gas Turbines Power*, **108**, 191 (1986).
30. Y. Solantausta, A. Oasmaa, K. Sipila, C. Lindfors, J. Lehto, J. Autio, P. Jokela, J. Alin and J. Heiskanen, *Energy Fuels*, **26**, 233 (2012).
31. T. S. Chan and M. C. Yuen, *J. Heat Transfer*, **112**, 1092 (1990).
32. J. Lehto, A. Oasmaa, Y. Solantausta, M. Kytö and D. Chiaramonti, Fuel Oil Quality and Combustion of Fast Pyrolysis Bio-oils, VTT Technology, VTT Technical Research Center, Finland (2013).